Dynamic Simulation of a Rotor System with Variable Speed

Mario Bischläger
Dipl.-Ing. / M.Sc.
TU Wien
Vienna, Austria

Christopher Gross
Dipl.-Ing. / M.Sc
Zoerkler Gears GmbH & Co KG
Jois, Austria

Jonas Koch
M.Sc
TU Munich
Munich, Germany

Agnes Poks
Dipl.-Ing. / M.Sc.
TU Wien
Vienna, Austria

Michael Weigand
Univ.-Prof. Dipl.-Ing. Dr.-Ing.
TU Wien
Vienna, Austria

ABSTRACT

Current concepts for fast rotorcraft and tiltrotor-/tiltwing aircraft require a speed variation in a wide range; this wide range cannot be covered by varying only the turbine speed. Such new aircraft under development require a rotor system with a large rotor speed variation but constant turbine speed which leads to the consequence that a transmission with a variable ratio during flight is necessary. TU Munich, TU Wien and Zoerkler gears work in the funded research projects VARI-SPEED and VARI-SPEED II on a solution "constant turbine speed / variable rotor speed" that consists of a transmission with variable ratio and a rotor system with rotor head and rotor blades for variable rotor speed. The helicopter UH-60A from Sikorsky Aircraft is used as reference.

The project VARI-SPEED showed the feasibility of a rotor system with variable speed. In the current project VARI-SPEED II the dynamic simulation of the system is built up. The paper describes the approach to the simulation and shows first results for each component. After completion of the simulation the elaborated rotor control will be implemented in a flight simulator for evaluation by pilots.

INTRODUCTION

Current Rotorcraft Developments like under the Future Vertical Lift Program in the US and RACER and NextGENCivil Tiltrotor in Europe deal with High-Speed Rotorcraft or Tiltrotor-/Tiltwing Aircraft which require a variable rotor speed either to adopt the rotor speed to high forward speed or to meet the different requirements of a rotor in Hover and Aircraft Mode of a Tiltrotor-/Tiltwing Aircraft. As the required speed range can not be covered by the turbine, TU Munich (Germany), TU Wien (Vienna, Austria) and Zoerkler Gears (Austria) work in thetransnational project "VARI-SPEED II" on a rotor system that can change the rotor speed via change of the ratio of the transmission (variable rotor speed with constant turbine speed). The project is based on the results of „VARI-SPEED“ and the direct follow-up project VARI-SPEED II VARI-SPEED showed that a rotor speed variation performed by a transmission system is possible. The efficiency and the flight envelope of the rotorcraft can be improved by this technology. Furthermore, a method for rotor blade design in a RPM range was invented. VARI-SPEED II will now build up a model of the complete dynamic system from engine to rotor of a helicopter with a variable speed rotor. This model will be used for dynamic simulations of the system. A scaled model of the module that changes the speed will be developed and pilot studies in a simulator are planned to find out the characteristics of such a system. Aim of the project is to reach TRL 3 as basis for further development of the technology with interested OEM´s.

Presented at the Vertical Flight Society's 78th Annual Forum & Technology Display, Ft. Worth, TX, USA, May 10-12, 2022,.

APPROACH

The focus of the project VARI-SPEED II is to investigate the interaction of the single components in the dynamic system, from the turboshaft engine to the rotor. An investigation of the loads of a single component is not possible any more because of the dynamics in the system and the different inertias of the components. It is essential to investigate the impact of the shifting process onto the dynamic system to understand and analyse its influence on the turboshaft engine and the rotor.

Another research question is dealing with the controllability and the handling qualities of a rotorcraft with rotor speed variation. Also failure scenarios, e.g. autorotation, are investigated. Stability and controllability criteria are quantified in simulations and should be enriched by the opinions of pilots which are testing the rotorcraft behaviour during simulator flights at TU Munich.

The third research question addresses the feasibility of the module that enables to vary the transmission ratio. The compound split gearbox and the variator are designed for scaled loads for later testing.

A controller for the output RPM is designed. It should be extended with an active vibration control system. Hardware components are defined for the controlling system and the demonstrator is designed. In addition a test schedule is created for the test in the following project.

RESULTS

Aero-Thermal Gas Turbine Model

The helicopter is driven by a pair of gas turbines GE T700-701C. The 1300 kW power-class two-shaft engine consists of a gas generator and a free power turbine (see Figure 1). A five-stage axial compressor with one final radial stage, the combustion chamber and the two-stage high pressure axial turbine build the gas generator. The two-stage free power turbine of axial type drives the rotor system of the helicopter through mechanical linkages and gears. Therefore, the free power turbine can be considered as part of the rotor system, to which it is mechanically linked. A freewheeling clutch allows the free power turbine to drive the rotor system but not vice versa. Further details of the engine can be found at the website of GE Aviation. In a preliminary study, the stationary design point data of the GE T700 gas turbine have been verified using the commercial software IPSEpro from SimTech Simulation Technology. The simplified thermodynamic model of the gas turbine neglects turbine cooling and compressor bleed air (see Figure 2). Output of the free power turbine is 1343 kW at a compressor pressure ratio of 17.5. The major part of the gas turbine engine work package is the development of an aero-thermal model of the gas turbine to describe the transient behaviour of the GE T700 engine. The model consists of a set of differential equations to describe the mass flow rate and power imbalances during transient operation and will be described briefly in the remaining part of this section.

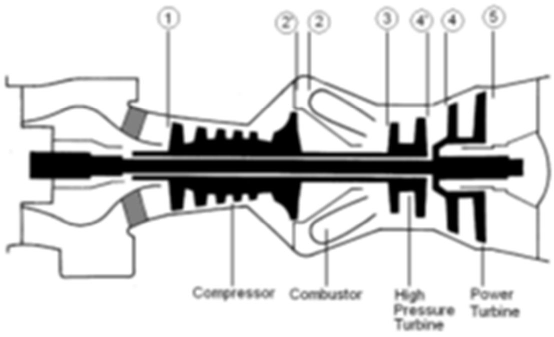

Figure 1. Principal cross section of GE T700 gas turbine engine (Ballin, 1988)

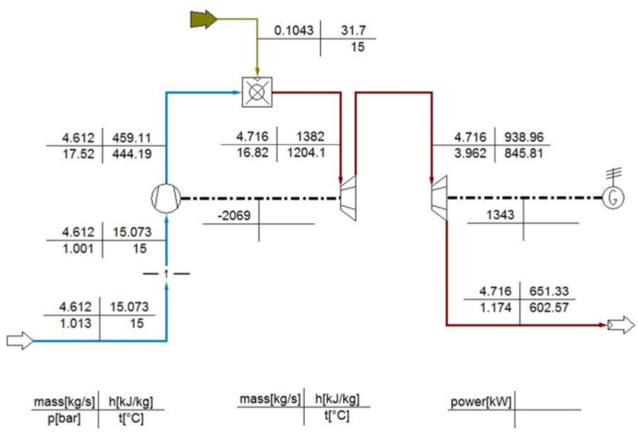

Figure 2. Design point thermodynamic model of GE T700 gas turbine engine in IPSEpro

Thermodynamic cycle calculations require values of specific heat at constant pressure at different temperatures and pressures. At typical working pressures in gas turbines, the influence of the pressure on the specific heat can be neglected and temperature has the major influence. In the present investigation, the method of Cumpsty and Marquis (Ref. 2) has been used to calculate values of specific heat at constant pressure. The empirical method provides data for mixtures of pure air and stoichiometric combustion gases of hydrocarbon fuel as a function of temperature and equivalence ratio. An important part of the model is the description of the turbomachinery components. Figure 3 shows the compressor map, which is the relation between corrected compressor mass flow rate and compressor pressure ratio at different corrected rotational speeds. Lines of constant corrected rotational speed (green) are from 65% to 100% gas generator design rotational speed of 44700 rpm. The data of the compressor map are adopted from Ballin (Ref. 1). The compressor operating range, limited by surge line (red) and choke line (cyan) is described by the so-called β-parameter according to Kurzke (Ref. 5). These are the black dotted lines in Figure 3. The free power turbine is represented by the relation of corrected mass flow rate and enthalpy difference according to Ballin (Ref. 1), whereas the gas generator turbine is treated as a choked nozzle.

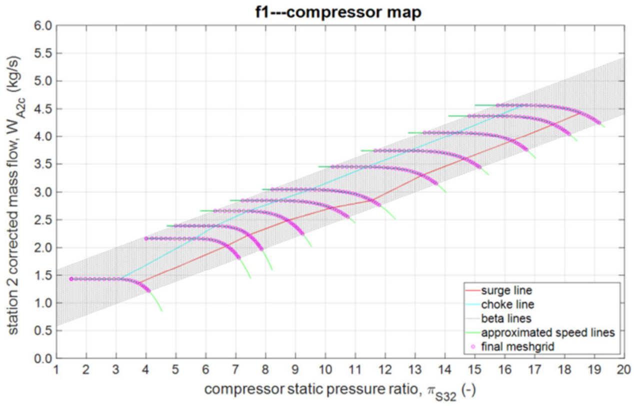

Figure 3: Compressor performance map

The combustion chamber is modelled taking into account the energy accumulation. Pressure and temperature in the combustion chamber are assumed to be constant and equal to their respective values at the outlet. Acceleration or deceleration of gas generator and free power turbine due to power imbalance during transients are modelled by conservation of angular momentum. This results in a set of two differential equations containing moments of inertia, rotational speeds and shaft power. Whereas the moment of inertia of the gas generator is constant, moment of inertia of the free power turbine depends on the operating state. This is due to the effect of the freewheeling clutch between gas turbine engine and helicopter rotor system. At the gas generator shaft, the power imbalance is a result of the power output of the high-pressure turbine and the power consumption of the compressor including friction losses. At the free power turbine shaft, the power imbalance results from the difference between power output of the free power turbine and the load requirement from the helicopter rotor system including friction losses, too. The final aero-thermal model of the gas turbine will be tested in an open-loop simulation to check steady state operating points. Furthermore, a fixed schedule of the fuel mass flow rate can be applied to increase the power output at constant rotational speed. The open-loop simulation is characterized by the fact that no control system is applied. In contrast, in a closed-loop simulation, the aero-thermal model of the gas turbine is linked with the control system. The objective of the control system is to keep the rotational speed of the free power turbine at a constant value of 20900 rpm. For example, if the torque requirement from the helicopter rotor system increases, the fuel mass flow rate has to increase. This causes changes of temperatures and pressures in the gas turbine process. Limiting values should guarantee that the gas turbine operates within a secure domain. The aero-thermal model will be able to incorporate these limits and provide them to the control system.

Transmission

As in the previous research, the drive train of the Sikorsky UH-60A helicopter was taken into account as a reference model. Figure 4 shows the arrangement of the original drive train of the UH-60A helicopter. Here, the power from the two turbo shaft engines (TSE) is transferred to the final planetary stage (PG) via an input module (IM) and a bevel gear (BG). The speed of the main rotor is almost constant throughout the flight.

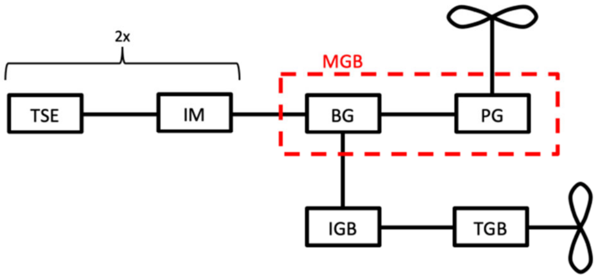

Figure 4: Arrangement of original drive train UH 60-A

As described in previous studies, an additional gear module is introduced to vary the speed, which is composed of a compound split (CS) and a variator module (VM) (Ref. 6,7). The speed can be varied by power split between compound split and variator witch are connected with an intermediate variator gearbox (VGB, see Figure 5 and Figure 6, red framed parts). Depending on where this additional gear group is introduced in the drivetrain, a distinction is made between two possible architectures:

In Architecture 1, the speed variation takes place after the bevel gear and before the final planetary stage, see Figure 5. In this arrangement, the additional gear group exists only once in the drive train, transmitting the power of both turbines.

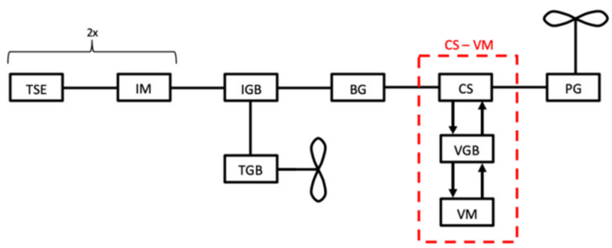

Figure 5: Architecture 1 with a compound split and a variator after the bevel gear

In contrast, in Architecture 2 the speed variation takes place before the bevel gear, see Figure 6. This has the consequence that the additional assembly only transmits the power of one turbine each, but is installed twice in the entire drivetrain.

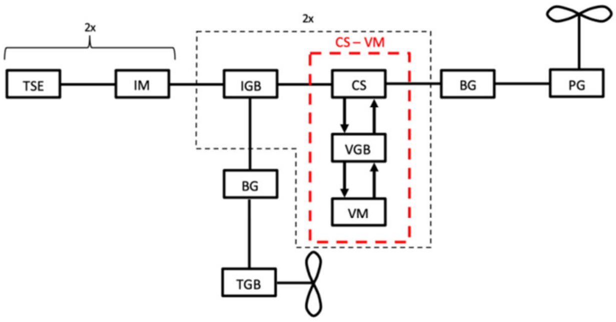

Figure 6: Architecture 2 with two compound splits and variators before the bevel gear

Within each of the two possible architectures, there are 4 different ways to arrange the planetary gears within the compound splits (Ref. 8). These 4 possible arrangements have been named with the letters A, B, C and D. There are 6 shafts per arrangement, and 2 of them are always coupled with each other.

Calculation

The optimum rotational speed range for speed variation is between 10% higher and 30% lower than the nominal speed (Ref. 9). To achieve this, a spread (maximum rotational speed / minimum rotational speed) of 1.5 was chosen. For the calculation, the transmission ratio of all stages of the main gearbox was set to slow (exclusive variator gearboxes, VGB). For cylindrical and bevel gear stages, this corresponds to a gear ratio >1 and for planetary gearsets to a gear ratio of >2.4 (fixed carrier ratio <-1.4, Ref. 6). Furthermore, the maximum speed of the compound split shafts was limited to 6000 rpm. This simplifies the selection of bearings and limits centrifugal forces. This selected rotational speed limit is based on the input speed into the main gearbox of 5750 rpm (Ref. 8). The share of tail rotor power was set at 15% of the total turbine power. In addition to the usual gear stages, a transmission is required between compound split and variator, the so-called variator gearbox (VGB).

The gearbox was calculated with these specifications. The aim was to find the transmission ratio combination of the different gear stages where the gearbox has the lowest mass. The calculation of the mass is based on formulas acc. to (Ref. 6) and depends on torque and the gear ratio. By means of moment equilibrium and variation of the transmission ratio of each stage (Ref. 8), the mass could be calculated. The calculation was carried out for the lowest rotational speed, as this is where the highest torques occur and therefore represent the critical load for the gearing. In addition, a further calculation was carried out in which the mass of all planetary gearsets was multiplied by a factor of 2.5. This factor resulted from a comparison between the calculation model and a detailed design (Ref. 8).

Results

Figure 7 and Figure 8 show the relationship between the gear mass and the minimum gear mass for the respective architectures. The x-axis shows the gear ratio of the planetary gearset directly in front of the main rotor and the y-axis shows the basic transmission ratio of the compound split. Since the total transmission ratio is constant at slow rotor speed, there is a corresponding transmission ratio of the bevel gear for each point. The right limitation of the results is due to the minimum bevel gear ratio of 1.

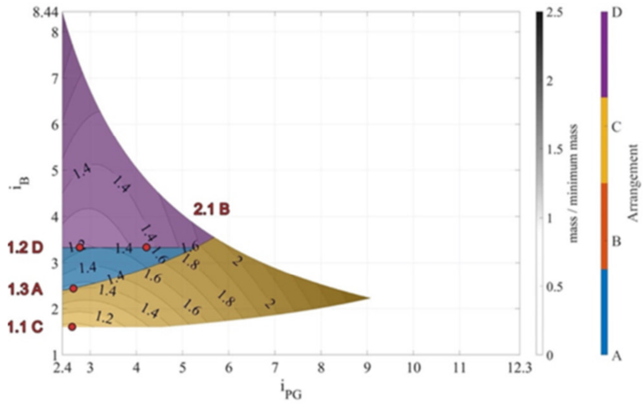

Figure 7: Architecture 1: minimum mass for all Arrangements

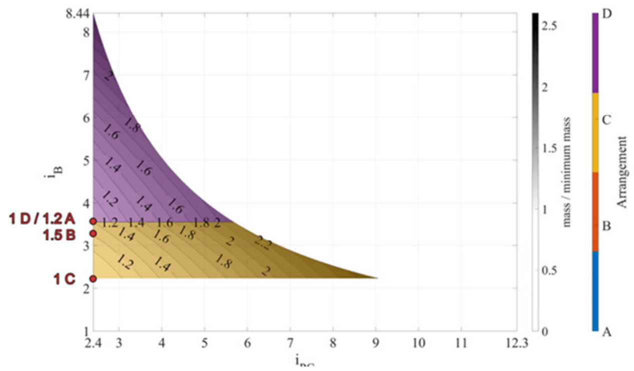

Figure 8: Architecture 2: minimum mass for all Arrangements

The lowest gear mass results from Architecture 2 with the arrangement C and D, which have approximately the same mass. Architecture 1 offers a solution with Arrangement C, which has a mass that is about 10% higher. The results shown include a factor of 2.5 for the mass of the planetary gears. All low mass solutions are at a low possible planetary gear and basic ratio of the compound split.

In Architecture 1, the compound split in the gearbox exists only once (Figure 5). This has the disadvantage that the entire power flow after the final planetary stage must be carried out again through the compound split and the bevel gear. In the latter case, this should be constructively possible, but in the case of the compound split, this results in the problem that it would have to be designed much larger than necessary in terms of strength, because the main rotor shaft has to be guided through the compound split (see Figure 9, left).

The Architecture 2 design has two compound splits (see Figure 6), but the power flow through the compound stage and the final planetary stage is similar to that of the original UH-60A gearbox. This means that the problem with the main rotor shaft does not occur (see Figure 9, right).

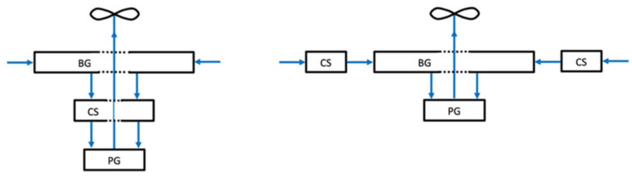

Figure 9: Power flow for Architecture 1 (left) and Architecture 2 (right)

The result of this work is that Architecture 1 turns out to be technically difficult to realize. This results from the previously mentioned facts that with this architecture the main rotor mast would have to be carried out by all parts of the compound split stages in front of it. In addition, the calculations also show the mass minima for Architecture 2.

Based on these findings, a dynamic simulation model is now to be created in order to further investigate its properties in a holistic dynamic simulation of the powertrain.

Variator

To vary the output speed of a drive, so-called power split gearboxes can be used. These consist of planetary gears. In a power split gearbox, the drive power, which in the case of VARI-SPEED II is provided by a gas turbine, is divided into a mechanical and a variator path. The variator path must contain a gearbox that can realize gear ratios between zero and infinity. This so-called variator is one of the key components for the successful development in VARI-SPEED II. In general, there are three ways to realize a gear ratio from zero to infinity

- Two hydraulic machines

- Two electric machines

- Mechanical IVT gearbox.

Power-split transmissions can be divided into three different variants. These are the input split, the output split and the compound split, shown in Figure 10. The difference between the three variants is the connection of the variator to the mechanical path.

In the output split, a portion of the input power is diverted through a fixed-ratio gearbox and fed to the variator. The power in the variator path is then fed to the planetary gearbox, with the fixed ratio i_0. In the planetary gearbox, the mechanical and variator paths are combined again. To change the speed at the output, the transmission ratio of the variator is controlled.

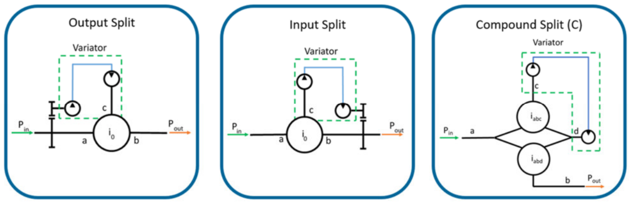

Figure 10: Power Split Transmissions

The input split can be seen as a mirrored output split. The input power is applied to shaft a, which is then split into the mechanical and variator paths via the planetary gear. After the speed in the variator path is changed, the two power paths are merged via a spur gear.

The major disadvantage of output and input split gearboxes is the poor efficiency when operating with gear ratios that deviate greatly from the mechanical point. To counteract this, a second planetary gear can be installed. If these two planetary gears are connected, the gearbox gets two degrees of freedom and two mechanical points. This design is called compound split. This principle is also used in hybrid vehicles. Depending on how the different shafts are connected, four different configurations (A, B, C, D) can result. For each of these four configurations, one can find optimal gear ratios of the two planetary gears for minimum mass.

The evaluation of the different technologies in terms of mass is based on the study by Amri et al. (Ref. 11) presented at the VFS Forum 2020. The investigated electric machines are based on electric car engines. In comparison to electric aircraft motors, these motors have a higher usable speed range which make them better suited as variators. The mass estimation of the individual technologies resulted in the lowest mass for the electric variator, with a small margin in front of the hydraulic variator. The mechanical variator, based on the NuVinci gearbox (Ref. 12), which was considered promising in advance, had a significantly higher mass. Therefore, this technology cannot be used in an aircraft.

Due to the poor performance of the mechanical variator, the efficiency evaluation was performed only for the electric and the hydraulic variator. Figure 11 compares these two technologies:

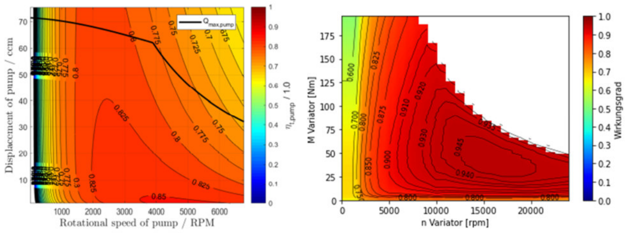

Figure 11 - Efficiency of hydraulic and electric variator

It can be seen that the electric machines, shown on the right, have a higher efficiency of up to 94.5%, compared to a maximum of 85% for the hydraulic machines (Ref. 13).

The final evaluation of the different technologies in terms of reliability, mass, efficiency, controllability and maintenance requirements showed that the development of an electric variator is the most promising. This result is further supported by the increasing importance of e-mobility.

Once the technology was selected, the variator could be sized. Based on the results of the compound split investigation, a variator was designed for the drivetrain in architecture 2, with 2 variable-speed modules upstream of the bevel gear stage. For this purpose, a simulation program was created to calculate the required power over the entire rotor speed range. Based on these power requirements, a permanent-magnet synchronous machine from the automotive sector was selected. This electrical machine is designed for high speeds and therefore has a high power density. In order to bring the speeds of the machine to the speed level of the variable speed module, a gearbox is required. Based on the machine data, the power to be applied by the generator including the losses in the variator train was calculated. These power requirements at full load are shown in Figure 12.

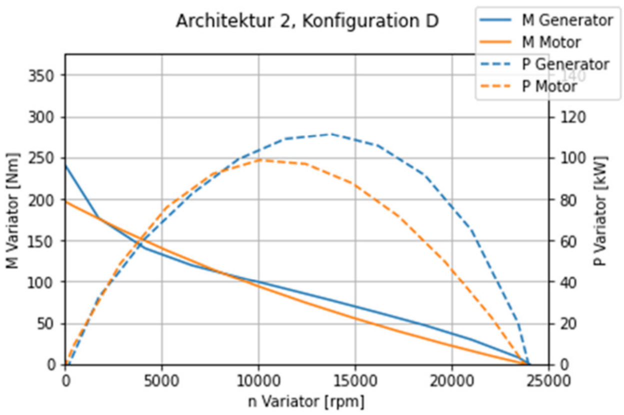

Figure 12 - Power requirements

With this electric machine selected, the total mass of the variators for both variable speed modules is 216 kg. This mass includes the required inverters and variator gearboxes. Over the entire speed range, at full load, there is a relatively constant power loss of 20 kW per variable-speed module, which must be dissipated by cooling.

One advantage of using electric variators is the possibility of temporarily storing surplus energy generated in the generator in an energy store. This energy can then be used to improve the performance of the helicopter in emergency situations. Various electrochemical and electrical storage technologies were evaluated for this purpose. The Li-ion battery was found to be the best concept. If the energy storage is used as an emergency system for engine failures and the like, only a small battery is needed. This concept has already been implemented by Airbus with the EBS system (Ref. 14). The use of the energy storage system for a hybrid drive is not yet possible with today's energy storage technologies.

In addition to speed variation, active vibration damping is another task to be performed by the variator. Here, the vibrations present in the entire drive train, including the rotor, are to be damped by an actuator. If a suitable control system is available, the electric motor in the variator train can be used directly as an actuator and no additional module is required. However, the motor and converter must have sufficiently high dynamics for this. In order to find out the exact requirements for the dynamics of the variator, further investigations must be carried out.

Rotor Simulation

The design of a rotor suitable for variable speed operation requires a detailed numerical model. The model must represent aerodynamic and structural elastic effects that occur due to the change in speed not only for quasi-steady flight conditions, but with emphasis on transient rotor speed maneuvers. These requirements motivate the use of the academic simulation environment Dymore (Ref. 15). It is a finite element based multibody dynamics code for the comprehensive modeling of flexible multibody systems, mainly used for rotorcraft and wind turbine investigation.

In the predecessor project VARISPEED I, possible gains in efficiency due to variable rotor speed have been examined for different helicopter configurations (Ref. 16. It turned out, that the UH-60 as a multi-purpose helicopter with a wide range of missions has great optimization potential. Due to the large mission shares of high and low blade loadings deviating from the design point $(C_T/\sigma)_{opt} = 0.09..0.1$, high power savings can be obtained by driving the blade loading towards the optimal design point though rotor speed adaption.
Focusing on the UH-60 helicopter, a multibody finite element model has been built up using Dymore (Ref. 17). It consists of the rotor blades, rotor blade attachments, pitch links, lag dampers, two scissors and the swash plate driven

by the forward, lateral and afterward servos. The model was validated for hover and straight-and-level forward flight conditions against wind tunnel data from the NASA Ames 80 x 120ft test facility and flight test data from the airloads flight test counter 85 (Ref. 18).

Since only the main rotor without the tail rotor is modeled, a trim strategy with neglect of the tail rotor forces is required. Therefore, the rotor is trimmed towards the lateral and longitudinal shaft bending moments and thrust. The trim target values are prescribed using UH60 test data from literature.

To identify the optimum rotor speed regarding the whole flight envelope of the helicopter, calculations were performed in VARISPEED I using NDARC (NASA Design and Analysis of Rotorcraft, Ref.. 19). The performance of trimmed steady-state flight conditions across the four dimensions flight speed μ, altitude h, gross weight m and rotor speed Ω was examined. One key finding is that the optimum rotor speed only depends on the blade loading $(C_T/\sigma)_{ref}$, i.e., a combination of gross weight (thrust) and altitude (density) (cf. eq (2)), and not on the two variables individually. This reduces the optimization problem to the 3D case.

The dependency on the blade loading is to be proven under use of Dymore. For better comparison of the performance characteristics under variable rotor speed, the rotor parameters are made independent of the actual rotor speed by normalizing them with the reference rotor speed $\Omega_{ref} = 27{,}02\,rad/s$. These parameters are denoted with the subscript $(..)_{ref}$:

$$\mu_{ref} := \mu \left(\frac{\Omega}{\Omega_{ref}}\right) \tag{1}$$

$$\left(\frac{C_T}{\sigma}\right)_{ref} := \frac{T}{\varrho\,\sigma\,A\left(\Omega_{ref}R\right)^2} = \frac{C_T}{\sigma}\left(\frac{\Omega}{\Omega_{ref}}\right)^2 \tag{2}$$

$$\left(\frac{C_P}{\sigma}\right)_{ref} := \frac{M\,\Omega}{\varrho\,\sigma\,A\left(\Omega_{ref}R\right)^3} = \frac{C_P}{\sigma}\left(\frac{\Omega}{\Omega_{ref}}\right)^3 \tag{3}$$

The power coefficient ratio $(C_P/\sigma)_{ref}$ is formed by calculating the shaftpower out of the shaftmoment M and the actual main rotor speed Ω, and subsequential de-dimensioning with the density ϱ, the rotor blade area σA, the rotor radius R and the reference rotor speed Ω_{ref}. With this, the power demand under variating rotor speed for one specific flight condition with $\left(\frac{C_T}{\sigma}\right)_{ref}$, μ_{ref} can be easily compared. Since the shaft moment is oscillating in forward flight condition (cf. fig. 16), the mean over several rotor revolutions is taken. Mind that the power coefficient only refers to the shaft power of the main rotor. Additional contributions from the tail rotor, gear losses and losses of the auxiliary aggregates are not considered.

Figures 13 and 14 show the power coefficient ratio in hover and forward level flight condition, respectively, at different rotor speeds and blade loadings. Consistent with the NDARC results, the Dymore simulations show the same dependence of optimum rotor speed (at minimum $(C_P/\sigma)_{ref}$) on blade loading. The more the blade loading decreases from the design point $(C_T/\sigma)_{opt}$, the more the rotor speed must be reduced.

Additionally, it is shown as expected from NDARC that the performance optimum is only dependent on the blade loading and not on the separate variables density and thrust. For this, two different simulations are performed with the same blade loading $\left(\frac{C_T}{\sigma}\right)_{ref} = 0.07$, but variated once with higher density $\left(\varrho = 1.28\frac{kg}{m^3}, T = 75{,}8kN\right)$ and once with lower thrust trim ($\varrho = 1.13\,kg/m^3, T = 67{,}0kN$). It can be seen that the power coefficient at varying rotor speed is almost identical for both cases.

Besides the simulation of steady-state flight conditions, the advantage of the Dymore model is the possibility to investigate transient maneuvers between different rotor speed states. Exemplarily, the rotor speed decrease from Ω_{ref} to $0.8 * \Omega_{ref}$ within $T = 10s$ is examined for forward flight condition with advance ratio $\mu_{ref} = 0.15$ and $(C_T/\sigma)_{ref} = 0.07$ (cf. fig. 3). The rotor speed change is prescribed under use of the cosine-function:

$$\Omega(\mathrm{t}) = \begin{cases} \Omega_1 & t \le t_1 \\ \Omega_1 + (\Omega_1 - \Omega_2) * \frac{1}{2}\left(1 - \cos\left(\pi\frac{t - t_1}{T}\right)\right) & t_1 < t < t_2 \\ \Omega_2 & t \ge t_2 \end{cases} \tag{4}$$

The corresponding shaft moment of the rotor speed transient is illustrated in Figure 16. The parabolic course arises from the correlation to the rotor acceleration over the principle of angular momentum. Since the thrust is kept constant by the trim routine via adjusting the blade pitch angle, the resulting shaft moment at $0.8 * \Omega_{ref}$ increases mainly due to higher induced drag.

The occurring shaftmoment oscillation is examined further by means of a Fourier analysis. Figure 17 shows the frequency spectrum of the shaftmoment at Ω_{ref}, belonging to the section between $t \in [1s; 2s]$. The two dominant frequencies appear at 4x and 8x of the rotor speed, corresponding to the number of blades $N_b = 4$.

The frequency analysis of the shaftmoment at $0.8 * \Omega_{ref}$ is illustrated in Figure 18, belonging to the section between $t \in [12s; 13s]$. Due to the deceleration of the rotor, the frequencies of 4/rev and 8/rev are shifted to the left. Still, the dominant frequencies of the shaftmoment correspond to these multiples of the rotor speed. Significantly, compared to Figure 19, the amplitude of the oscillations increases for both frequencies. This indicates an operation closer to the resonance frequencies of the rotor, mainly driven by lead-lag and flap modes.

The isolated consideration of rotor shaft torsional vibrations without the powertrain contribute to a better understanding of torsional vibrations occurring in the coupled rotor-gear-turbine-model. This becomes relevant since an active vibration control system is to be developed for the coupled simulation.

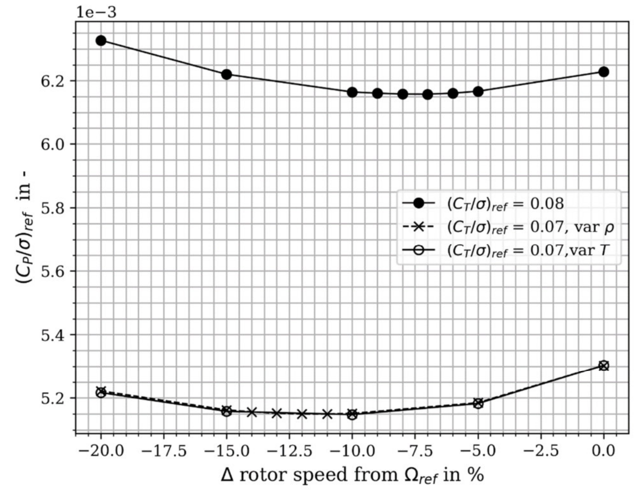

Figure 13. Power coefficient in hover

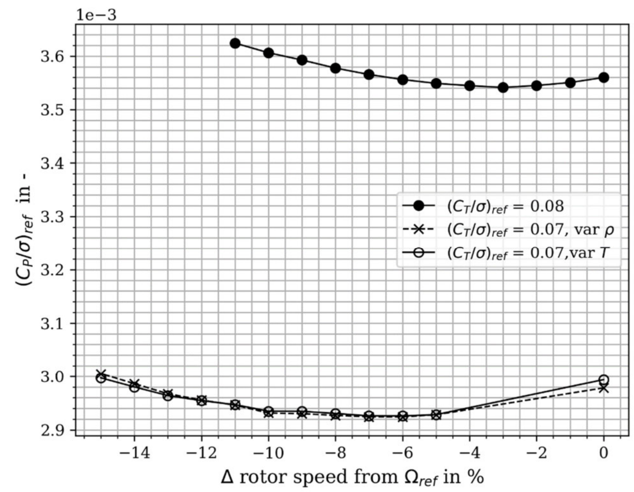

Figure 14. Power coefficient in forward flight at μ_{ref} = 0.15

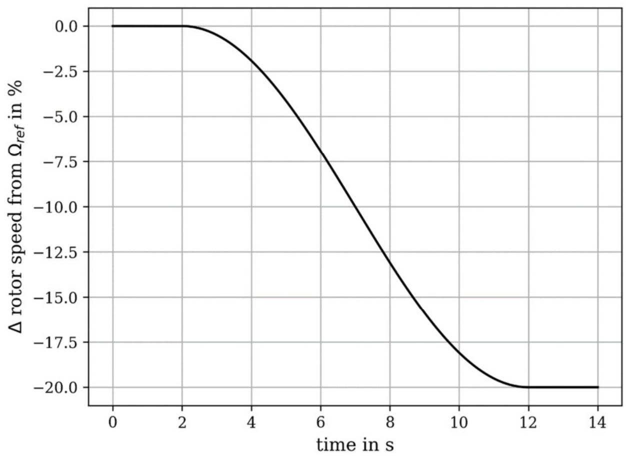

Figure 15. Rotor speed transient

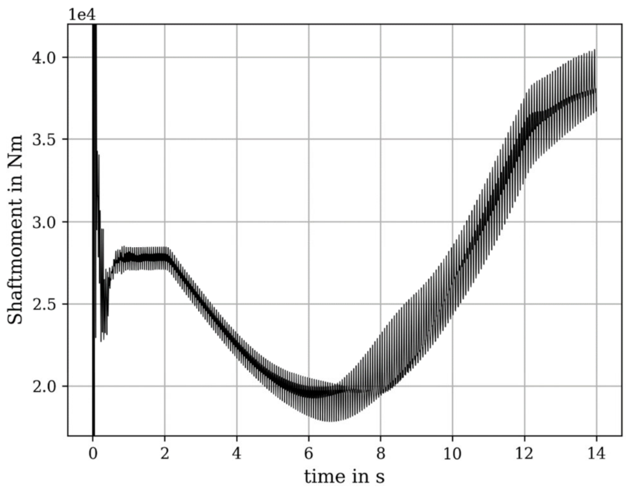

Figure 16. Shaft moment transient

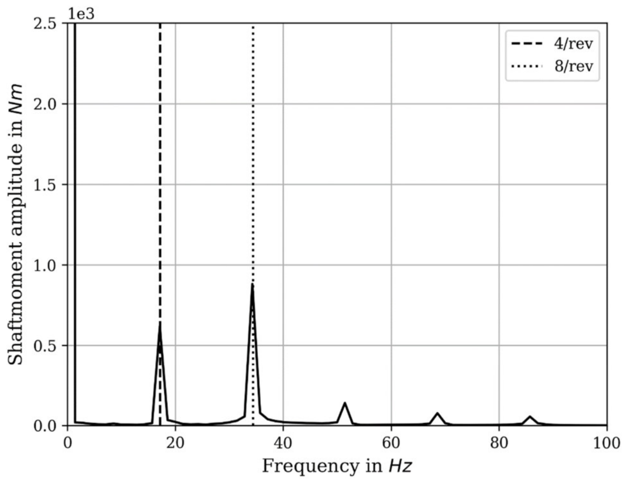

Figure 17. FFT of shaft moment at Ω_{ref}

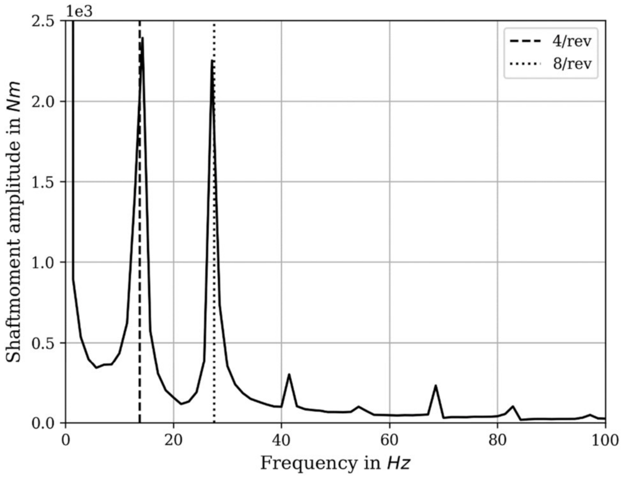

Figure 18. FFT of shaft moment at $0.8 * \Omega_{ref}$

The fully coupled dynamic system, including the whole drivetrain and full flight physics model of the UH-60A, will be used to conduct a pilot-in-the-loop test campaign at the Rotorcraft Simulation Environment (ROSIE). ROSIE is a fixed-base pilot-in-the-loop rotorcraft simulator at the chair of Helicopter Technology at the Technical University of Munich (TUM). ROSIE features a high-fidelity visual system and an original BO-105 cell and cockpit, as shown in figure 1. The visual system consists of a 5 meter diameter hemispherical dome with a 6-channel 4k@120hz projection system. The cockpit's inside features the original controls of the BO-105 as well as a Primary Flight Display (PFD) and a Multifunctional Display (MFD) showing a digital moving aeronautical map, see figure 2. Helicopter dynamics models are hosted in a Matlab/Simulink framework and are easily exchangeable.

Figure 19: TUM Rotorcraft Simulation Environment

Figure 20: Display configuration

Rotor Control Design

The presented design for a rotor speed variation of a helicopter performed by a transmission system shows its advantages in higher efficiency and dynamic. An innovative control topology will be invented to exploit the full potential of this improved rotor technology. Similar to a hybrid powertrain of an automotive, the turbine is coupled over a compound split gearbox with electric drives, which apply a time-varying rotor torque, as shown in Figure 21.

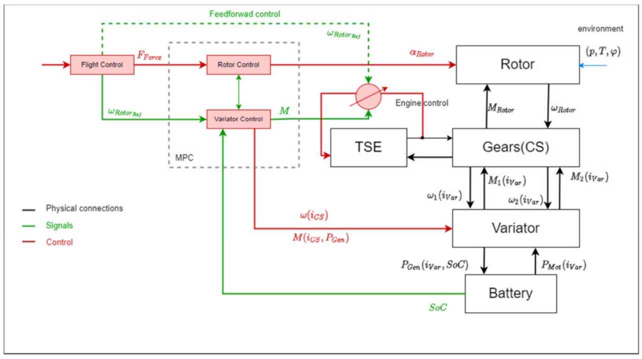

Figure 21: Control structure for vibration damping (VR) and energy management (EM)

As shown in the Figure, a two-degree-of-freedom controller determined the optimal reference trajectory generated by the pilot input. The increased degrees of freedom provide the controller with an energy-optimal-engine speed. Additionally, active damping reduces the vibrations that are cause by the elastic rotor components, see Ref. 20. Different methods like the robust control method and optimal control theory are explored to effectively compensate torsional vibrations of the rotor, see Ref. 21 and Ref. 22.

The combination of the optimal operating point of the variators regarding efficiency and constraints for temperature and speed/torque is calculated offline and stored in maps that are used for the feedforward control (Ref. 23).

The feedback DOF is assigned the task of torsional vibration suppression, which is solved by an adaptive model predictive controller.

To formulate an optimal predictive controller, a model that shows the vibration characteristic of the system has to be designed. Since the real-time capability is essential for the controller, the strongly nonlinear helicopter dynamics have to be simplified. The simplified model that is based on Ref. 24 is obtained through lumping rotational inertias and springs. It consists of a two-shaft engine with a gas generator and a free power turbine, gearbox, compound split with variators, and a transmission shaft, which forms a rotor drive train system together.

The parametrization of the model is based on the detailed UH-60 helicopter model, which was built as a multibody finite element model that has been built in Dymore (Ref. 25).

The nonlinear dynamic model is expressed as following:

$$\dot{x} = f(x, u, \boldsymbol{\theta})$$
$$y = g(x, u, \boldsymbol{\theta})$$

The model consists of the input, output, and state variables with a time-varying parameter vector $\boldsymbol{\theta(t)}$. The time-varying parameter vector obtains the different dynamic characteristics of the helicopter in terms of the two-shaft engine with variable rotor speed and different gear ratios.
To obtain a real-time capable model, linearization and discretization around the desired operating point (x_0, u_0) are performed. The Taylor series approximation is shown in the following equation:

$$\begin{cases} \dot{x} = f\,(x, u, \boldsymbol{\theta}) \approx f\,(x_0, u_0) + \dfrac{\partial f}{\partial x}|_{(x_0,u_0)}(x - x_0) + \dfrac{\partial f}{\partial u}|_{(x_0,u_0)}(u - u_0) \\ y = g\,(x, u, \boldsymbol{\theta}) \approx g\,(x_0, u_0) + \dfrac{\partial g}{\partial x}|_{(x_0,u_0)}(x - x_0) + \dfrac{\partial g}{\partial u}|_{(x_0,u_0)}(u - u_0) \end{cases}$$

The shown Taylor series expansion neglect derivatives above first order.

The linearized model depends on the time-varying parameter θ and can rewritten in the state-space formulation:

$$\Delta\dot{x} = \mathbf{A}(\theta)\Delta x + \mathbf{B}(\theta)u$$
$$\Delta y = \mathbf{C}(\theta)\Delta x$$

Based on the developed model, an adaptive Model Predictive Control (MPC) is chosen and can be formulated as an optimization problem with horizon length m. Main advantage of the MPC is the optimal trajectory following with respect to all system constraints. Also, the decoupling function is a main benefit of this controller architecture. The objective function and necessary constraints are based on the Ref. 26 and is described as following

$$min\ J = \sum_{i=1}^{m} \omega_1 \left(\frac{Q_E[k+i] - Q_H[k+i]}{Q_{E,ds}} \right)^2 + \sum_{i=1}^{m} \omega_2 \left(\frac{N_P[k+i] - Q_H[k+i]}{Q_{E,ds}} \right)^2$$

$$s.t. \begin{cases} W_f^{min} \le W_f[k+i] \le W_f^{max} \\ \alpha_c^{min} \le \alpha_c[k+i] \le \alpha_c^{max} \\ \omega_{1,2}^{min} \le \omega_{1,2}[k+i] \le \omega_{1,2}^{max} \\ SoC^{min} \le SoC[k+i] \le SoC^{max} \\ |\Delta W_f[k+i]| \le \Delta W_f^{max} \qquad i = 1,2,\ldots,m \\ |\Delta\alpha_c[k+i]| \le \Delta\alpha_c^{max} \\ N_p^{min} \le N_p[k+i] \le N_p^{max} \\ \alpha_c[k+i] \le \alpha_c^{max} \\ S_m[k+i] \ge \alpha_c^{max} \end{cases}$$

The flight control provides an optimal trajectory in response of the pilot input, based on which the MPC performs an optimal trajectory calculation of the load change. The developed adaptive predictive control design decides whether energy should be stored to the battery, passed through the variator directly, or whether additional energy from the battery storage is required. Furthermore, the transmission control holds constraints, prevents the engine from over-temperature, and avoids peak loads to extend the system lifetime.

The overall developed structure combines the innovative engine design with a robust and modern predictive optimal controller.

CONCLUSIONS

The project VARI-SPEED showed the feasibility of a rotor system with variable speed. In VARI-SPEED II the dynamic simulation of the system is built up. The paper describes the approach to the simulation and shows first results for each component. After completion of the simulation the elaborated rotor control will be implemented in a flight simulator for evaluation by pilots.

ACKNOWLEDGMENTS

The project VARI-SPEED II is a transnational research project, funded in Austria by TakeOff (Federal Ministry of Climate Action, Environment, Energy, Mobility, Innovation and Technology) and in Germany by LuFo, the Federal Aviation Research Programme (Federal Ministry for Economic Affairs and Climate Action).

REFERENCES

1. Ballin M.G. “A High Fidelity Real-Time Simulation of a Small Turboshaft Engine”. *NASA Technical Memorandum 100991* (1988)

2. Cumpsty N.A., Marquis A.J., “An Approximate Method to Obtain Thermodynamic Gas Properties for Use in Gas Turbines”. *ASME Paper GT2014-26205* (2014)

3. GE Aviation: https://www.geaviation.com/military/engines

4. SimTech Simulation Technology: https://www.simtechnology.com

5. Kurzke J. "How to get Component Maps for Aircraft Gas Turbine Performance Calculations". *ASME Paper 96-GT-164* (1996)

6. Amri, H., Hartenthaler,K., Weigand, M., „Mass and Kinematic Analysis of Compound Split with Simulation of the Shifting Process for Variable Rotor Speed" American Helicopter Society 74th Annual Forum Proceedings, Phoenix, AZ, May 2018

7. Paschinger, P., Amri, H., Hartenthaler, K., Weigand, M., „Compound Split Drivetrains for Rotorcraft" 43rd European Rotorcraft Forum Proceedings, Milan 2017, p. 1127–1141

8. Amri, H., Donner, F., Huber, F., Weigand, M., „Mass Optimisation of Variable Rotor Speed Compound Split Drivetrains for Rotorcraft" 45th European Rotorcraft Forum Proceedings, Warszaw 2019, p. 1127–1141.

9. Garre, W., Pflumm, T., Hajek, M., 42nd European Rotorcraft Forum Proceedings, Lille 2016, p. 717–721.

10. Stevens, M.A., Handschuh, R.F.m Lewicki, D.G. "Concepts for Variable/Multi-Speed Rotorcraft Drive System" American Helicopter Society 46th Annual Forum Proceedings, Montreal, May 2008,

11. Amri, H., Donner, F., Braumann, L., Huber, F., Weigand M., "Comparison of Variator Technologies for Variable Rotor Speed Drivetrains". American Helicopter Society 76th Annual Forum Proceedings, Virtual, October 2020

12. Braumann, Lorenz, *„NuVinci Getriebe im Leistungsverzweigten Getriebe"*. Diploma Thesis, TU Wien, 2020.

13. Paschinger, P., "*Development and Dynamic Simulation of a Variable-Ratio Transmission System for the UH-60 Helicopter"*. PhD Thesis, TU Wien, 2019.

14. Airbus Helicopters starts flight tests with engine back-up system. https://www.airbus.com/en/newsroom/press-releases/2021-09-airbus-helicopters-starts-flight-tests-with-engine-back-up-system. (Online, 09. 11 2021.)

15. Bauchau, Bottasso, and Nikishkov, "Modeling Rotorcraft Dynamics with Finite Element Multibody Procedures" *Mathematical and Computer Modelling*, 2001.

16. Garre, W., Pflumm, T., and Hajek, M. "Enhanced Efficiency and Flight Envelope by variable Main rotor speed for different helicopter configurations" . 42nd European Rotorcraft Forum Proceedings, Lille 2016

17. Rex, W., Pflumm, T., and Hajek, M., "UH-60A Rotor and Coupled Rotor-Fuselage Simulation Framework Validation and Analysis". 45th European Rotorcraft Forum Proceedings, Warszaw 2019

18. Yeo, Bousman, and Johnson, "Performance Analysis of a Utility Helicopter with Standard and Advanced Rotors," *Journal of the American Helicopter Society*, 2004

19. Johnson, W., "NDARC-NASA Design and Analysis of Rotorcraft Theoretical Basis and Archtecture", AHS Aeromechanics Specialists Conference. San Francico 2010

20. Vadamalu, Raja Sangili , Beidl, Christian, "MPC for Active Torsional Vibration Reduction of Hybrid Electric Powertrains", *IFAC-PapersOnLine,* Volume 49, Issue 11, 2016, Pages 756-761, ISSN 2405-8963

21. Kozek, Martin, and Schirrer, Alexander, "Modeling and control for a blended wing body aircraft. Advances in industrial control". *Springer International Publishing Cham*, 2015. 1-308.

22. Vadamalu, Raja Sangili , Buch, David, Xiao, Hong, Beidl, Christian, "Energy management of hybrid electric powertrain using predictive trajectory planning based on direct optimal control" *IFAC-Papers OnLine*, Volume 48, Issue 25, 2015, Pages 236-241, ISSN 2405-8963, http://dx.doi.org/

23. Tang, Xiaolin, Yang, Wei, Hu, Xiaosong, Zhang, Dejiu, "A novel simplified model for torsional vibration analysis of a series-parallel hybrid electric vehicle" *Mechanical Systems and Signal Processing*, Volume 85, 15 February 2017, Pages 329-338, ISSN 0888-3270

24. Hopkins, S.A., Ruzicka, G.C., Ormiston, R.A., "Analytical investigations of coupled rotorcraft/engine/drive train dynamics". Proceedings of the American Helicopters Society 2nd International Aeromechanics Specialists Conference. Bridgeport, C.T. 1995

25. Rex, W., Pflumm, T, Hajek, M., "UH-60A Rotor and Coupled Rotor-Fuselage Simulation Framework Validation and Analysis". 45th European Rotorcraft Forum Proceedings, Warszaw 2019

26. Wang, Yong et.al., "Research on predictive control of helicopter/engine based on LMS adaptive torsional vibration suppression". *Journal of Low Frequency Noise, Vibration and Active Control* 37.4 (2018), p.1151-1163